Novel Electronic Structure of Inhomogeneous Quantum Wires on a Si Surface

H. S. Yoon, S. J. Park, J. E. Lee, C. N. Whang, and I.-W. Lyo*

Atomic-scale Surface Science Research Center and Institute of Physics and Applied Physics, Yonsei University, Seoul 120-749, Korea

(Received 10 November 2003; published 2 March 2004)

A one-dimensional system of Si(111)-(5 × 2)-Au is explored using scanning tunneling microscopy and spectroscopy. The chain of Si adatoms called bright protrusions (BP's) is found to be semiconducting with an evanescent state in the gap, which originates from adjoining metallic BP-free segments. A quantitative analysis shows that the evanescent state decays in inverse-Gaussian form, leading to an appearance of a parabolic BP chain, and scales to its chain length. Spatial decay of the state suggests a quadratic band bending and the existence of a Schottky-like potential barrier at the interface driven by charge transfer.

DOI: 10.1103/PhysRevLett.92.096801 PACS numbers: 73.20.At, 68.37.Ef, 73.30.+y

Low dimensional materials are fascinating because of their unique electronic properties and possible device applicability. Metal in semiconductor systems is particularly suitable because of the ease to fabricate low dimensional structures with tailored electronic properties. Recently, Au/Si(111) systems have drawn a lot of interest because of the suggestion of unusual ground states. A one-dimensional metallic band observed on a highly stepped Si(111) has been proposed to have spin-charge separation, indicating evidence of the Luttinger liquid [1]. For the realization of this state, a Peierls instability has to be overcome to avoid metal-insulator transitions such as the one found in Au/Si(557) [2]. On the other hand, Si(111)-(5 × 2)-Au, which should be metallic by electron counting [3], was suggested to have such a Peierls gap in the one-dimensional band to explain the disappearance of the band near E_F. Here the existence of a Peierls gap was attributed to the doubling of the periodicity to 5 × 2 from 5 × 1 with an otherwise half-filled Au-induced band. However, the energy gap of 0.3 eV is too large for a Peierls gap; thus, the origin of the disappearance of the band near E_F remains unknown [4].

Si(111)-(5 × 2)-Au is a self-organized, one-dimensional system with the two rows of dimerized substitutional Au chains along $[1\bar{1}0]$ [5,6]. Although these rows are not imaged, scanning tunneling microscopy (STM) reveals a reconstructed surface with a complex structure: Unique to this surface are randomly distributed short chains of Si adatoms called bright protrusions (BP's), spaced in units of four lattice constants of a Si(111) surface, rendering the local periodicity to 5 × 4 [7–11], and best described as a lattice fluid [12,13]. Despite being a key to the understanding of the Au/Si(111) system, atomic-scale studies of the electronic structure of these chains have been lacking until recently [14,15].

In this Letter, we explore the Si chain structure on a Si(111)-(5 × 2)-Au surface at low temperature (78 K), where the stability and energy resolution of STM are much improved. We find the one-dimensional system consists of a series of alternating metallic and semiconducting segments, and surprisingly an atomic-scale analogy of a Schottky barrier is formed at the interfaces. This highly unusual system may serve as a new basis for understanding highly disordered one-dimensional metallic systems, and also may explain why the one-dimensional band of Si(111)-(5 × 2)-Au disappears near E_F in photoemission.

A clean Si(111) surface was obtained from a wafer vicinally oriented by 4° toward the $[11\bar{2}]$ direction, by flashing it to 1500 K. Au was deposited from a tungsten filament at 940 K at a rate lower than 0.01 ML/s, and the surface quality was monitored by low energy electron diffraction. All preparation was performed in an ultrahigh vacuum condition with base pressure below 7×10^{-11} mbar. STM measurements were performed at base pressure below 3×10^{-11} mbar and at liquid nitrogen temperature. I/V measurements were made for up to 20 s over individual sites to enhance the statistics, during which the drift rate was kept to lower than 0.03 nm/min.

Figure 1(a) represents a typical image of Si(111)-(5 × 2)-Au decorated by partially ordered bright adatomlike features called BP's. A BP chain consists of a series of integer multiples of a local structural unit marked by the square brackets in Fig. 1(b), which includes a BP and a pair of "ears." The measured width of the unit along $[1\bar{1}0]$ is 1.54 nm, corresponding to $4a_0$ where a_0 is the lattice constant of the (111) plane. The ears are spaced uniformly by $2a_0$. Surprisingly, as shown in Fig. 1(b), a BP chain at +0.3 eV exhibits a dramatic variation of about 0.15 nm with the innermost unit of a BP chain lying lowest in the topographic height. The effect is confined within the BP chain characterized by a dark region, separated from neighboring parallel rows by Au rows. This "chaining" of BP's is observed for all $4a_0$ spaced BP chains involving more than two BP's, and broken only by BP spacings larger than $4a_0$. For instance, the arrow in Fig. 1(b) points to a $6a_0$ wide spacing between BP's, which contains the shortest BP-free segment of length $2a_0$ with an ear. Line profiles of the BP

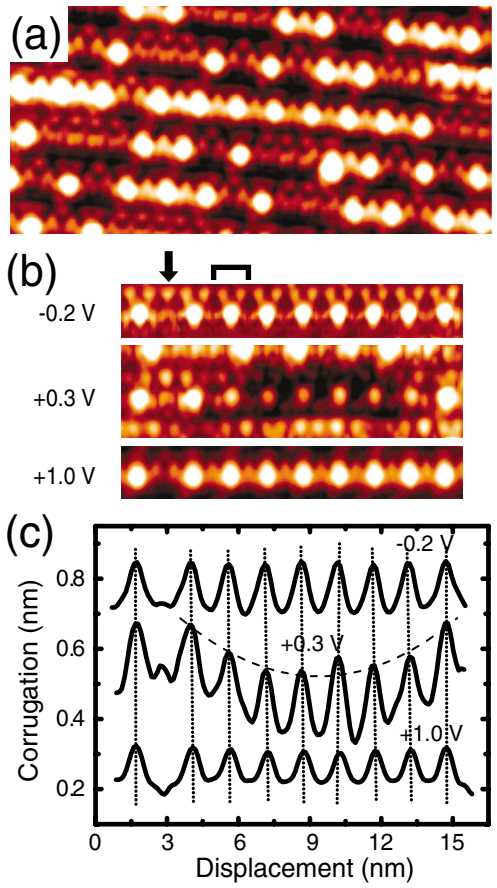

FIG. 1 (color online). (a) A 7.5×10.5 nm^2 STM image of typical Si(111)-(5×2)-Au at $V_{sample} = +0.8$ V and $i_t = 0.05$ nA, and (b) bias-dependent STM images of a 8 BP long, $4a_0$ spaced chain and a $6a_0$ BP-free segment (arrow). The bracket in (b) denotes a local unit cell of a BP chain, with a BP and a pair of less bright "ears." (c) Vertically aligned line cross sections of the chain at corresponding biases are shown, with a parabolic fit to a +0.3 eV case. A small deviation of the fourth BP from the right side is due to a defect on the lower row.

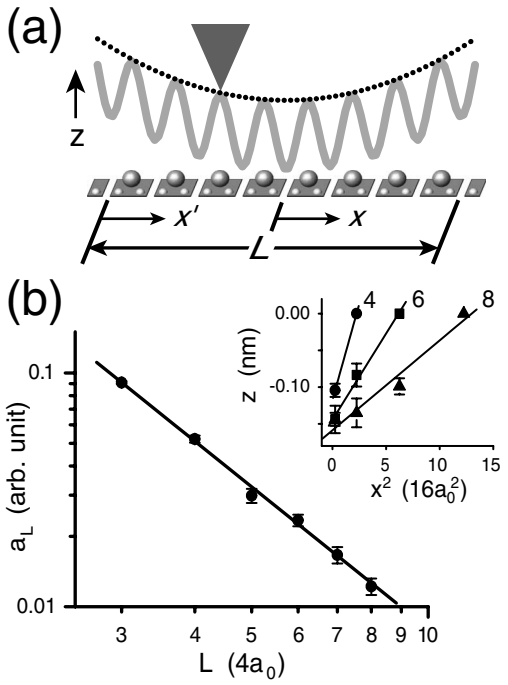

FIG. 2. (a) A diagram of a parabolic envelope of the tip trajectory under a constant current mode. Each plate with one large and two small balls represents a local unit cell depicted in Fig. 1(b). (b) A log-log plot of normalization constant a_L vs length L of BP chains. The inset displays z positions of BP's in each chain as a function of x^2, with x and z as defined in (a). The number next to each fit is the length of the BP chain in units of $4a_0$.

chain in Fig. 1(c) show that the envelope of corrugation of BP's measured at +0.3 eV is parabolic, while those at −0.2 and +1.0 eV show small variations. Clearly this is an electronic effect because this behavior is observed only near E_F, between −0.2 and 0.8 eV. Note that the corrugation of each BP is constant throughout within a chain, indicating that not just BP but also the substrate itself is subjected to the same effect.

For a further analysis, z positions of each BP in BP chains were measured and plotted as a function of the distance from the center of each chain, as shown in the inset of Fig. 2(b). Linear fits to the z positions in x^2 show good agreement, indicating that the envelopes of BP chains are, indeed, parabolic in a form of $a_L x^2$ where a_L represents a curvature of a BP chain with chain length $L = 4a_0 n_{BP}$ with n_{BP} being the number of BP's in the chain. A log-log plot of thus obtained slopes a_L versus chain length L gives an excellent linear fit, as shown in Fig. 1(b), with a slope -2.0 ± 0.1, or $a_L \propto L^{-2.0\pm0.1}$. This means that all BP chains are scaled by their own chain lengths with a characteristic scaling factor η, so that $a_L = \eta/L^2$. As an immediate consequence, the maximum height difference in a BP chain is fixed to $\sim$0.15 nm, regardless of length L, as can be verified from the inset of Fig. 2(b).

In order to understand this unique behavior of a one-dimensional BP chain, high resolution scanning tunneling spectroscopy was performed over BP chains. The results on a typical five BP long chain and an adjoining BP-free segment are shown in Fig. 3. It was found that the spectra vary little within a local unit cell, while the cell-to-cell variation dominates, consistent with an almost rigid parabolic shift of BP's and substrate shown in Fig. 1(b). The labeling of peaks was based on normalized dI/dV spectra and associated local density of states (LDOS) maps (not shown). Among them, restatomlike states A and A' are found along β, as indicated in Fig. 3, near the midsection of local unit cells, while delocalized states B and C run parallel along α and γ, respectively. Details will be described elsewhere [16].

Normalized I/V spectra in Fig. 3 clearly show that the intensity of state C strongly depends on the location

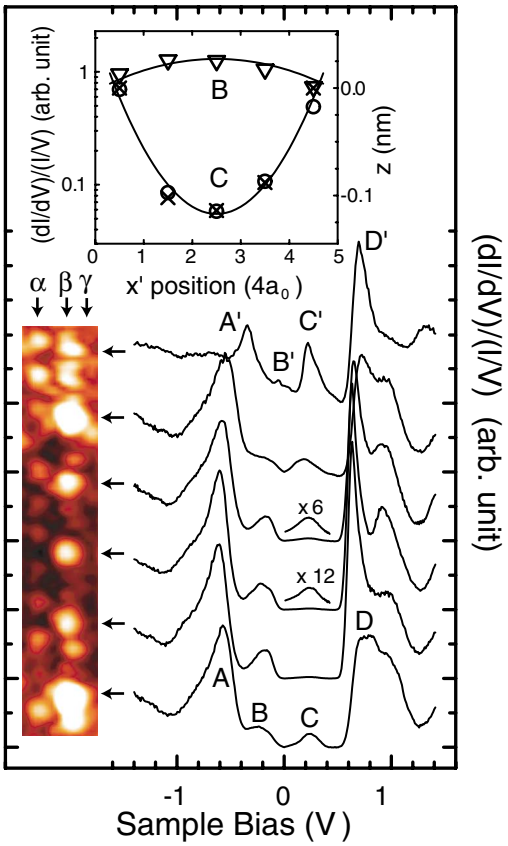

FIG. 3 (color online). A STM image of a chain with 5 BP's and their corresponding normalized dI/dV spectra at the site of each BP (lower 5 curves), and at a BP-free segment (top curve), taken at $V_{\text{sample}} = -1.5$ V and $i_t = 1.0$ nA. Long ticks on the y axis denotes $(dI/dV)/(I/V) = 0$. The inset is a plot of z positions of 5 BP's in the chain ($\times$), in comparison with the log of the peak intensities at states B ($\triangledown$) and C ($\bigcirc$). Z positions of state B and C were rigidly shifted for the best fit. α, β, and γ denote locations within local unit cells, running parallel to Au rows.

within a chain: The farther out in the chain it lies, the greater intensity it has. Within the Tersoff-Hamann model, the relation between this position dependent LDOS and the z-position variation of a BP chain can be understood. At a low bias, the tunneling current i_t can be approximated by an equation, $i_t \sim \rho_C(x)\exp(-2\kappa z)$, where ρ_C and κ represent LDOS at state C and the extinction coefficient, respectively. If κ is independent of x, a constant tunneling current mode of STM follows the relation $\ln\rho_C \propto z$. Comparison between the log of the normalized dI/dV and the z position of each BP in the chain is shown in the inset of Fig. 3, giving a remarkable agreement between the two. Also shown in the inset is that of state B, which exhibits the spatial variation opposite to state C: It is strongest in the middle and weakest at the ends of a BP chain. This strongly suggests that the z-position variation of a BP chain is solely due to the change in LDOS of each state. In other words, the parabolic z variation of the tip is not caused by a spatially varying κ. As κ is a slow varying function of bias, any dependence of κ on x would have been reflected similarly for both states. As the inset of Fig. 3 indicates, however, this is not the case.

Taken together with our earlier observation of the self-scaling of the parabolic z variation of the BP chain, it is clear that the LDOS of state C is an inverse Gaussian, $\rho_C(x) \propto \exp\{\eta(x/L)^2\}$, where the origin of x is at the middle of a BP chain, as defined in Fig. 2(a), and η represents the lateral scaling factor of LDOS. For a constant tunneling current condition, we obtain the relation $d(x/L)^2/dz \propto 2\kappa/\eta$, and by fitting to the experimental data, we found $\eta/\kappa = 16 \pm 2$ Å. Normalized dI/dV data in Fig. 3 provides further determination of η, since the functional form of $\rho_C(x)$ is now known. A parabolic fit to the normalized dI/dV data in Fig. 3 gives $\eta = 14.7 \pm 1.2$. When substituted in the earlier result on η/κ, we obtain the result $\kappa = 0.92$ Å^{-1}, which is quite reasonable, in view of a typical value of 1.0 Å^{-1} at surface [17]. Thus, our analysis method, although very simple, allows independent determinations of constants such as κ and η.

At this point, it would be fruitful to discuss the physical origin of such a LDOS variation. A clue to the question can be obtained from the spectra in Fig. 3, where the BP-free region (top curve) is metallic due to state B' lying across E_F, while the BP chain is semiconducting with a gap of ~0.6 eV. Comparison of corresponding states in each region shows that states in metallic segments are shifted to higher binding energies by 0.24, ~0.2, and ~0.1 eV for states A, B, and D, respectively, with the notable exception of states C and C' staying identical among each other. On the other hand, state D follows the variation of state B in such a way that its LDOS variation cancels out z variations of BP's caused by state C above +0.8 eV.

Diminishing LDOS of state B near the interface of metallic and semiconducting segments indicates that charge is transferred from state B in a BP chain to the adjoining BP-free segments. It appears that restatomlike state A' acts as a primary charge trap, aided by the absence of Si adatoms in BP-free segments. A similar behavior of restatoms has been found in a clean Si(111)-(7 × 7) surface, where the amount of charge in dangling bonds of Si adatoms depends on the density of neighboring restatoms [18]. At the same time, there is also substantial intercell charge transfer suggested by a fully empty C' state, and negligible LDOS of state C in the middle of a BP chain. Thus, state C may be regarded as an evanescent state, originating from the strong C' state in a neighboring BP-free unit, and decaying into the energy gap of the BP chain, with its decay rate dictated by scaling factor η.

A direct consequence of having an evanescent state is that an infinite chain of BP's would then have a true gap above E_F due to the complete lack of C' states. This idea

was put to a test as follows: A postdeposition of Si on top of the initially prepared Si(111)-(5 × 2)-Au was found to increase the BP density to the extent that all of the available $4a_0$ sites are occupied [19]. It was found that the resulting BP-saturated surface not only had a true gap, but also defied all attempts to image the surface at state C, lending support to our charge transfer model [16].

Lateral transfer of charge is bound to cause band bending. The binding energy shifts ranging from ~0.1 to 0.24 eV found earlier may be partly caused by the band bending, although the varying amounts of chemical shift in each state make it difficult to determine the size of band bending accurately. Nevertheless, consistent chemical shifts suggest that the band of a BP chain bends downward away from the interface.

The remarkable form of one-dimensional LDOS thus found in finite BP chains severely limits the choice of possible potentials that state C is subjected to. It is easy to show that an inverse-Gaussian form of evanescent wave functions is possible in a gap only if the conduction band edge (CBE) varies quadratically, namely, like a harmonic potential. Thus, the very existence of the inverse-Gaussian form of LDOS is a strong argument favoring band bending. Furthermore, a simple s-wave simulation indicates that the evanescent state should lie ~0.3 eV below CBE, giving a qualitative agreement with the current position of the gap whose upper edge is assigned to the position of state D. On the other hand, the influence of the interface dipole on a band bending potential is comparable to the lateral dimension of the junction. The effect of the zero-dimensional interface to the potential then decays away as z^{-2} in one-dimensional wires [20], opening another possibility for the inverse-Gaussian dependence. Although understanding the precise nature of the interface requires further exploration, we conclude that the atomic-scale analogy of Schottky barrier may exist between a semiconducting BP chain and an interfacing metallic BP-free segment.

Random distribution of BP chains may affect the band structure. Photoemission shows that a strongly dispersive Au-induced surface state begins to disappear at about 0.3 eV below E_F and upwards, coincident with the appearance of state B [3]. On the other hand, unlike the state B located at α, state A located at β apparently does not influence the Au-induced surface state. This indicates that the Au-induced surface state may be in spatial proximity to row α and that spatially varying chemical environments such as state B cause the spectral weight of the Au-induced surface state to be spread over the energy range ~0.3 eV of state B. This kind of spatial inhomogeneity may also be responsible for a similar observation made on a photoemission peak in Au/Si(335)-Na that disappears near E_F with no dispersion [21].

In summary, we found a novel one-dimensional electronic structure made of serially alternating metallic and semiconducting segments at an atomic scale. Above E_F, a metallic segment induces an inverse-Gaussian evanescent state in the gap of a nearest-neighbor semiconducting chain. The evanescent state scales to its own chain length, with a scaling factor $\eta = 14.7 \pm 1.2$, and an extinction coefficient $\kappa = 0.92$ Å^{-1}. Its functional form suggests, as a CBE, a harmonic potential centered at the middle of a BP chain and, consequently, the formation of atomic-scale Schottky barriers at both interfaces of the chain. Intralocal and interlocal unit cell charge transfer is suggested as the origin of the LDOS variation of a BP chain and band bending, as well as the evanescent wave. The interaction of randomly distributed state B with the Au-induced surface state may cause the disappearance of the band near E_F in photoemission.

The authors are grateful to M. H. Kang and H.W. Yeom for helpful discussions. They acknowledge support by KOSEF through ASSRC, and by MOST through National R&D Project for Nano Science and Technology.

*Electronic address: lyo@yonsei.ac.kr

[1] P. Segovia, P. Purdie, M. Hengsberger, and Y. Baer, Nature (London) **402**, 504 (1999).
[2] J. R. Ahn, H.W. Yeom, H. S. Yoon, and I.W. Lyo, Phys. Rev. Lett. **91**, 196403 (2003).
[3] R. Losio, K. N. Altmann, and F. J. Himpsel, Phys. Rev. Lett. **85**, 808 (2000).
[4] K. N. Altmann *et al.*, Phys. Rev. B **64**, 035406 (2001).
[5] S. M. Durbin, L. E. Berman, and B.W. Batterman, Phys. Rev. B **33**, 4402 (1986).
[6] L. D. Marks and R. Plass, Phys. Rev. Lett. **75**, 2172 (1995).
[7] A. A. Baski, J. Nogami, and C. F. Quate, Phys. Rev. B **41**, 10 247 (1990).
[8] J. D. O'Mahony *et al.*, Phys. Rev. B **49**, 2527 (1994).
[9] T. Hasegawa and S. Hosoki, Phys. Rev. B **54**, 10 300 (1996).
[10] T. Hasegawa, S. Hasaka, and S. Hosoki, Surf. Sci. **357**, 858 (1996).
[11] M. Shibata, I. Sumita, and M. Nakajima, Phys. Rev. B **57**, 1626 (1998).
[12] Y. Yagi, K. Kakitani, and A. Yoshomori, Surf. Sci. **356**, 47 (1996).
[13] A. Kirakosian *et al.*, Phys. Rev. B **67**, 205412 (2003).
[14] M.-H. Kang and J.-Y. Lee, Surf. Sci. **531**, 1 (2003).
[15] S. C. Erwin, Phys. Rev. Lett. **91**, 206101 (2003).
[16] H. S. Yoon *et al.* (to be published).
[17] J. Tersoff and N. D. Lang, *Scanning Tunneling Microscopy*, edited by J. A. Strocio and W. J. Kaiser (Academic Press, San Diego, 1993), p. 1.
[18] R. Wolkow and P. Avouris, Phys. Rev. Lett. **60**, 1049 (1988).
[19] A. Kirakosian *et al.*, Surf. Sci. **532**, 928 (2003).
[20] F. Léonard and J. Tersoff, Phys. Rev. Lett. **84**, 4693 (2000).
[21] P. Starowicz *et al.*, Phys. Rev. Lett. **89**, 256402 (2002).